

GENTLE AND VIOLENT GOLD INTERACTIONS FROM THE BNL AGS

INGVAR OTTERLUND

*Division of Cosmic and Subatomic Physics, University of Lund,
Solvegatan 14, S-223 62 Lund, Sweden*

EMU01 Collaboration

M. I. Adamovich, M. M. Aggarwal, Y. A. Alexandrov, N. P. Andreeva, Z. V. Anzon, R. Arora, F. A. Avetyan, S. K. Badyal, E. Basova, K. B. Bhalla, A. Bhasin, V. S. Bhatia, V. G. Bogdanov, V. I. Bubnov, T. H. Burnett, X. Cai, I. Y. Chasnikov, L. P. Chernova, M. M. Chernyavsky, G. Z. Eligbaeva, L. E. Eremenkov, A. S. Gaitinov, E. R. Ganssauge, S. Garpman, S. G. Gerassimov, J. Grote, K. G. Gulamov, S. K. Gupta, V. K. Gupta, H. Huang, B. Jakobsson, L. Just, S. Kachroo, G. S. Kalyachkina, E. K. Kanygina, M. Karabova, G. L. Kaul, S. Kitroo, S. P. Kharlamov, S. A. Krasnov, V. Kumar, P. Lal, V. G. Larionova, V. N. Lepetan, L. S. Liu, S. Lokanathan, J. Lord, N. S. Lukicheva, S. B. Luo, T. N. Maksimkina, L. K. Mangotra, N. A. Marutyan, N. V. Maslennikova, I. S. Mitra, S. Mookerjee, H. Nasrulaeva, S. H. Nasyrov, V. S. Navotny, J. Nystrand, G. I. Orlova, H. S. Palsania, N. G. Peresadko, N. V. Petrov, V. A. Plyushchev, D. A. Qarshiev, W. Y. Qian, Y. M. Qin, R. Raniwala, S. Raniwala, N. K. Rao, N. Saidkhanov, N. A. Salmanova, L. G. Sarkisova, V. R. Sarkisyan, G. S. Shabratova, T. I. Shakhova, S. N. Shpilev, D. Skelding, K. Soderstrom, Z. I. Solovjeva, E. Stenlund, E. L. Surin, L. N. Svechnikova, K. D. Tolstov, M. Tothova, M. I. Tretyakova, T. P. Trofimova, U. Tuleeva, S. Vokal, J. Vrlakova, H. Q. Wang, Z. Q. Weng, R. J. Wilkes, Y. L. Xia, G. F. Xu, D. H. Zhang, P. Y. Zheng, S. I. Zhokhova and D. C. Zhou
Alma Ata-Beijing-Chandigarh-Changhsa-Dubna-Jaipur-Jammu-Kosice-Linfen-Lund-Marburg-Moscow-Seattle-St Petersburg-Tashkent-Wuhan-Yerevan

Invited talk at the Symposium on Heavy-Ion Physics at the AGS:
HIPAGS '93, 13-15 January 1993, MIT, Cambridge, MA, USA.

CERN LIBRARIES, GENEVA

CERN LIBRARIES, GENEVA



CM-P00063046

GENTLE AND VIOLENT GOLD INTERACTIONS FROM THE BNL AGS

INGVAR OTTERLUND

*Division of Cosmic and Subatomic Physics, University of Lund,
Solvegatan 14, S-223 62 Lund, Sweden*

EMU01 Collaboration

M. I. Adamovich, M. M. Aggarwal, Y. A. Alexandrov, N. P. Andreeva, Z. V. Anzon, R. Arora, F. A. Avetyan, S. K. Badyal, E. Basova, K. B. Bhalla, A. Bhasin, V. S. Bhatia, V. G. Bogdanov, V. I. Bubnov, T. H. Burnett, X. Cai, I. Y. Chasnikov, L. P. Chernova, M. M. Chernyavsky, G. Z. Eligbaeva, L. E. Eremenkov, A. S. Gaitinov, E. R. Ganssauge, S. Garpman, S. G. Gerassimov, J. Grote, K. G. Gulamov, S. K. Gupta, V. K. Gupta, H. Huang, B. Jakobsson, L. Just, S. Kachroo, G. S. Kalyachkina, E. K. Kanygina, M. Karabova, G. L. Kaul, S. Kitroo, S. P. Kharlamov, S. A. Krasnov, V. Kumar, P. Lal, V. G. Larionova, V. N. Lepetan, L. S. Liu, S. Lokanathan, J. Lord, N. S. Lukicheva, S. B. Luo, T. N. Maksimkina, L. K. Mangotra, N. A. Marutyan, N. V. Maslennikova, I. S. Mittra, S. Mookerjee, H. Nasrulaeva, S. H. Nasyrov, V. S. Navotny, J. Nystrand, G. I. Orlova, H. S. Palsania, N. G. Peresadko, N. V. Petrov, V. A. Plyushchev, D. A. Qarshiev, W. Y. Qian, Y. M. Qin, R. Raniwala, S. Raniwala, N. K. Rao, N. Saidkhanov, N. A. Salmanova, L. G. Sarkisova, V. R. Sarkisyan, G. S. Shabratova, T. I. Shakhova, S. N. Shpilev, D. Skelding, K. Soderstrom, Z. I. Solovjeva, E. Stenlund, E. L. Surin, L. N. Svechnikova, K. D. Tolstov, M. Tothova, M. I. Tretyakova, T. P. Trofimova, U. Tuleeva, S. Vokal, J. Vrlakova, H. Q. Wang, Z. Q. Weng, R. J. Wilkes, Y. L. Xia, G. F. Xu, D. H. Zhang, P. Y. Zheng, S. I. Zhokhova and D. C. Zhou
Alma Ata–Beijing–Chandigarh–Changhsa–Dubna–Jaipur–Jammu–Kosice–Linfen–
Lund–Marburg–Moscow–Seattle–St Petersburg–Tashkent–Wuhan–Yerevan

ABSTRACT

Au+Au and Au+Ag interactions are studied at 11.6 A GeV/c. Results on projectile fragmentation and on particle densities and their fluctuations are presented.

1. Introduction

One of the highlights during 1992 was the realization of gold beam experiments at the BNL/AGS. This was the first time that nuclear interactions induced by gold nuclei could be studied at such high energies as 10.7 A GeV. The EMU01 collaboration exposed both stacks and chambers. The work with scanning and measurements is in progress and some results have already been obtained.

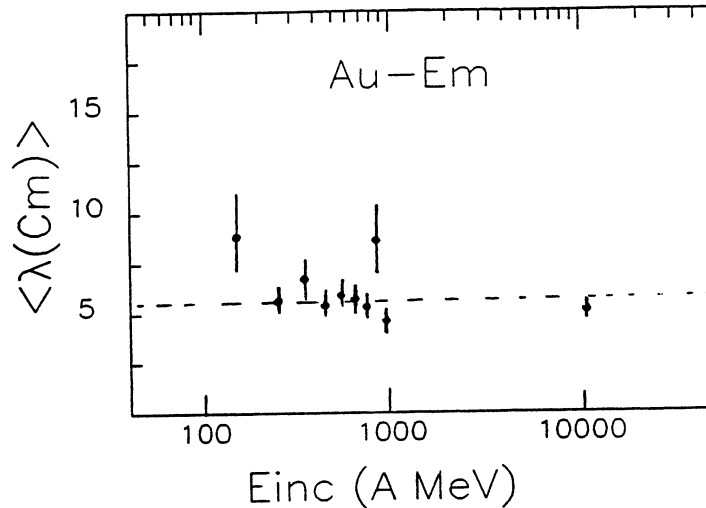


Fig. 1: The mean free path of Au-nuclei in nuclear emulsion.

So far we have been focusing on two topics; projectile fragmentation and particle densities in the most violent collisions. The characteristics of Au+Em interactions can be directly compared with those predicted from interactions by lighter nuclei (^{16}O , ^{28}Si and ^{32}S) at different energies.¹ They can also be compared with results from Au+Em interactions at lower (LBL) energies reported by Waddington and Freier². Although the data presented here are statistically limited and preliminary they do exhibit comparatively energy independent mean multiplicities of projectile fragments, complete destruction of the Au nuclei in central collisions and complexity in He-fragment emission. The particle densities and their fluctuations are to a large extent given by stochastic emission from the participants and by fluctuations in the number of participants.

2. The Mean Free Path

In the stacks each incident Au-nuclei were followed along the track. In Fig. 1 the mean free path is compared to corresponding values at lower energies measured by Waddington and Freier². The results is consistent with being energy independent. The very thick Au-tracks in emulsion makes it difficult to detect small interactions in which only a few particles are released from the projectile. Therefore the minimum bias sample of interactions could be lacking events with small projectile break up.

3. Rapidity and Pseudorapidity

The BNL/AGS gold beam has a kinetic energy of 10.7 A GeV. The nucleon-nucleon centre of mass rapidity for this incident energy is $y_p/2=1.6$ and the beam pseudorapidity η_p is 3.29, i.e. slightly larger than the beam rapidity 3.2. As long as we are treating data from fixed target experiments, pseudorapidity distributions are very good approximations of rapidity distributions, at least for pions, the only major difference being a shift of about one quarter of a unit in rapidity. From FRITIOF-generated samples of central S+S interactions at 200 A GeV the difference ($\langle \eta \rangle - \langle y \rangle$) was found to be 0.24.³ Therefore we expect the peak in the η -distribution for symmetric collisions, η_{peak} , to appear at:

$$\eta_{peak} = y_p/2 + 0.24 = 1.84 \quad (1)$$

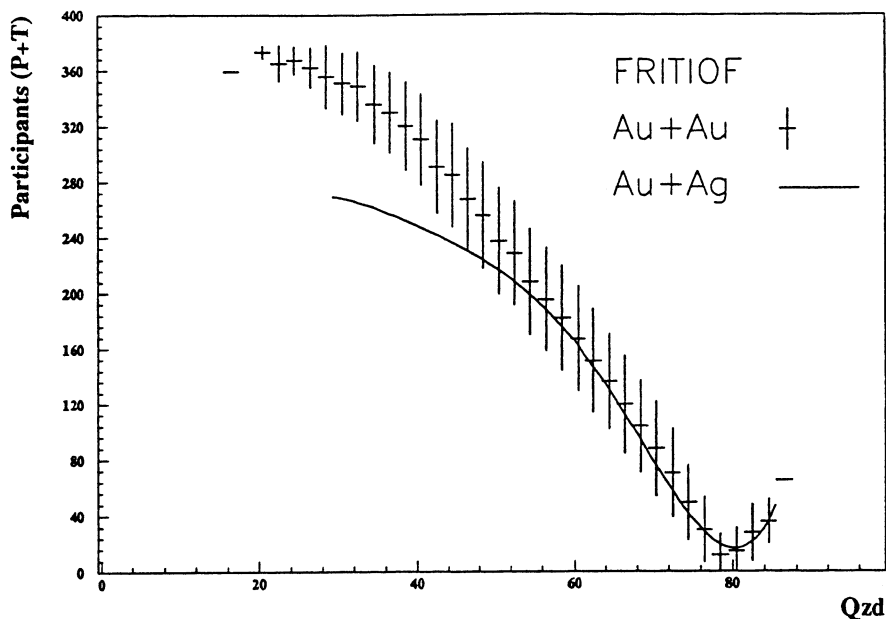


Fig. 2: The number of participating nucleons as a function of Q_{ZD} .

The charge flow in the forward direction, Q_{ZD} , has been measured in order to select central interactions. At 11.6 A GeV/c the opening angle of the forward cone, $\theta_{Q_{ZD}}$, inside which all charges are counted giving Q_{ZD} , is 2.98° . This value corresponds to $\eta=3.65$. Fig. 2 shows the number of participants, P , from the target and projectile in Au+Au and Au+Ag interactions estimated as a function of Q_{ZD} from the geometry in FRITIOF⁴. η -distributions measured in central Au+Au and Au+Ag collisions at 11.6 A GeV/c with, $Q_{ZD} < 40$, are discussed in Section 9.

4. Topology

Waddington and Freier² have studied interactions in emulsion irradiated with gold nuclei at 990 A MeV. Because Au-nuclei with such low incident energy slow down and stop in the emulsion, interactions in the energy range ≤ 900 A MeV were available for measurements. At these low energies they found that the gold nuclei are essentially never broken up into just nucleons and helium nuclei, even in collisions with Ag or Br targets. Only 1.3 ± 0.1 % of the interactions have no fragment with $Z \geq 3$ emerging from the projectile nucleus while 50 % produce two or more such fragments. We observe that at 11.6 A GeV/c the Au-nuclei are completely broken up into nucleons in ~ 4 % of the Au+Au interactions.

Waddington and Freier² found that the total charge emitted on fragments with ($Z \geq 3$), Z_f , exhibits a strong energy dependence in the energy range 100-900 A MeV. It was however observed that although Z_f decreases with energy, the mean number of individual fragments with $Z \geq 3$, $\langle n_f \rangle$, is essentially independent of energy. They found $\langle n_f \rangle$ to be 2.02 ± 0.27 . This value is very similar to the value 1.9 ± 0.1 observed by us at 11.6 A GeV/c.

Waddington and Freier² also observed that the charge carried by helium fragments, Z_α , is weakly energy dependent, increasing from 3.5 to 5.0 He-fragments per interaction when the energy increases from 150 to 900 A MeV. In Fig. 3 the multiplicity of He-fragments, $\langle n_\alpha \rangle$, is compared to corresponding multiplicities observed by Waddington and Freier²

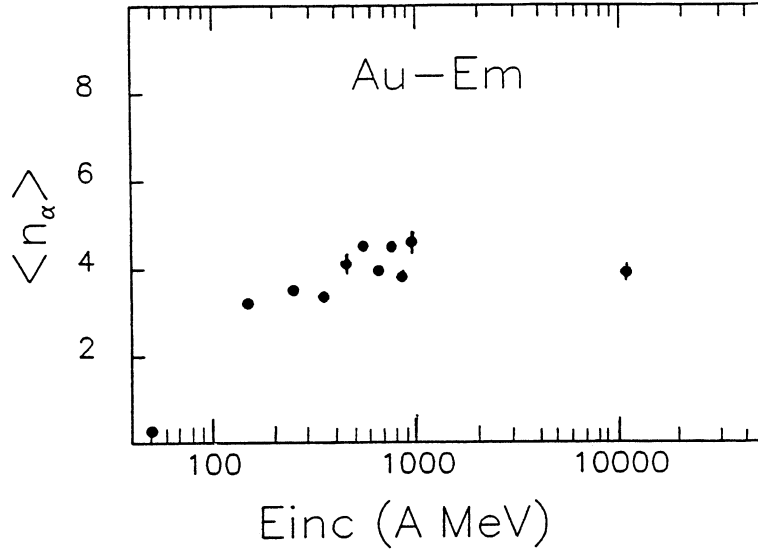


Fig. 3: Mean multiplicities of He-fragments as a function of energy.

at lower energies. The values are similar.

5. Two Components in the He-particle Angular Distribution

Fig. 4 shows the projected angular distribution (θ_{proj} -distribution) of He-fragments associated with the projectile. The distribution is described by two Gaussians. Thus the logarithmic value of the yields, plotted as a function of θ_{proj}^2 , disentangles into two linear distributions as seen in Fig. 4. The σ -values, given in Fig. 4, are determined under the assumption that the He-emitting sources are moving with the same velocity as the projectile gold nuclei. The high σ -value of the tail-distribution tells us that there is a sideward communication between the participant and spectator matter. This will slow down the spectator fragments and the assumption, that the He-emitting source moves in the beam direction with the velocity of the incident gold nuclei, is then of course wrong.

6. The Multiplicity of Produced Particles per Participant

The energy dependence of the ratio between the multiplicity of produced particles and the number of participants is exhibited in Fig. 5 for different min. bias samples. On the abscissa the corresponding multiplicity in pp collisions are used instead of energy. Data from different colliding systems, at the same incident energy, fall on top of each other and a linear dependence is observed.

$$\langle n \rangle / P = 0.734 \cdot n_{ch} - 1.44 \quad (2)$$

We can easily predict the total number of produced particles for any system by just estimating the number of participating nucleons for the trigger used. At 11.6 A GeV/c we find $\langle n \rangle / P = 1.085$ and for 300 participants, which is a typical value for our central gold-gold interactions, we thus expect the mean multiplicity of produced particles to be about 325.

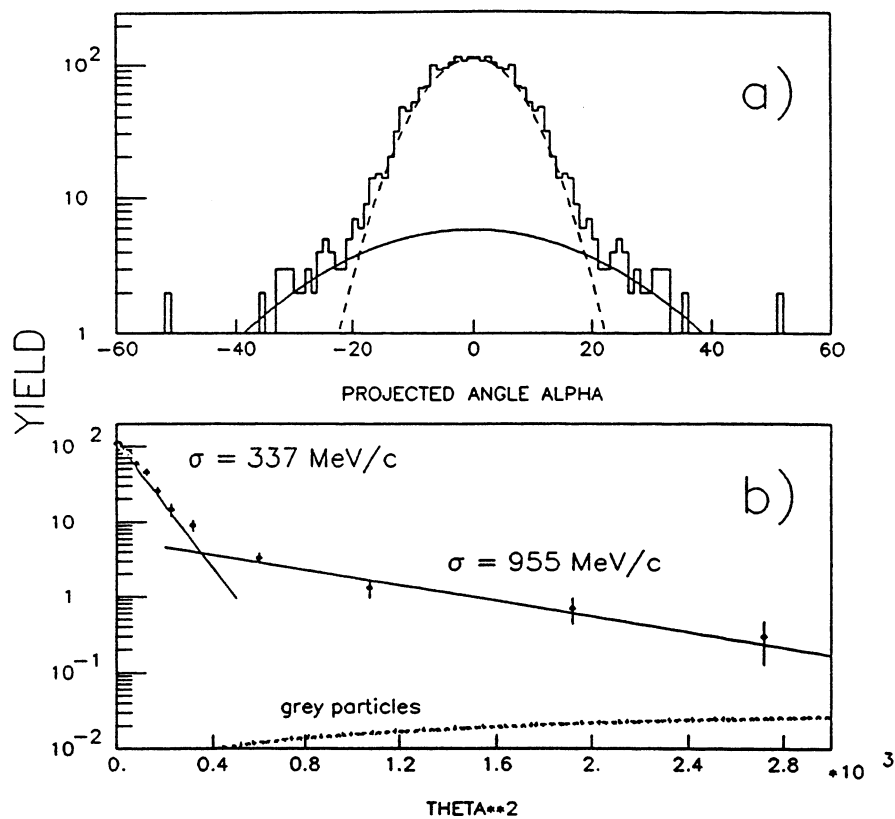


Fig. 4: Projected angular distributions of He-fragments. a) θ_{proj} -distribution. b) The logarithmic value of the yields as a function of θ_{proj}^2 .

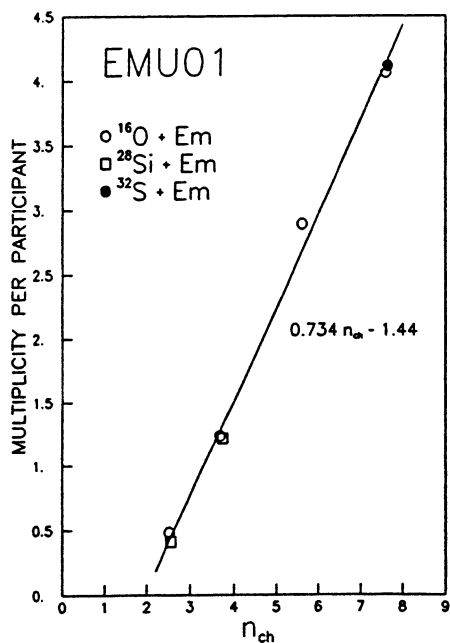


Fig. 5: The linear relationship between the multiplicity of produced particles per participant, $\langle n \rangle / P$, and the multiplicity from pp collisions, n_{ch} , at the corresponding energy.

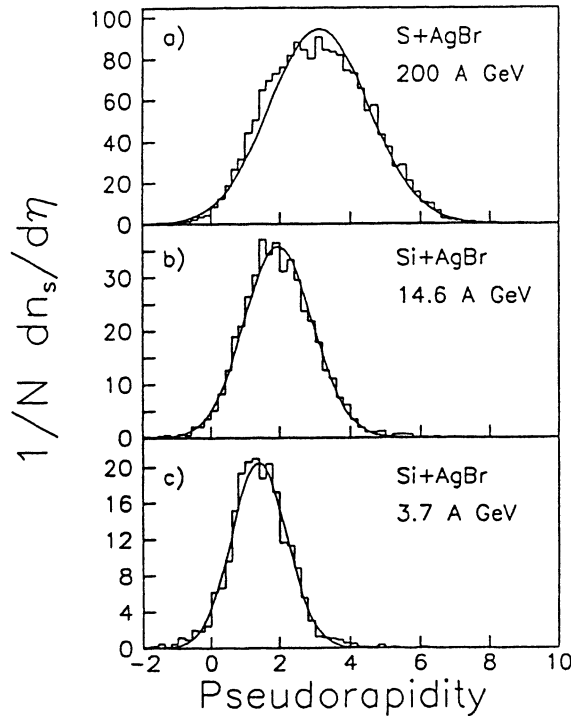


Fig. 6: Examples of pseudorapidity distributions for central events and the corresponding Gaussian fits.

7. Systematics of Pseudorapidity Distributions

Pseudorapidity distributions of produced particles from various interacting systems at different energies have been parametrized using Gaussian fits.¹ Examples of pseudorapidity distributions for central events and corresponding Gaussian fits are shown in Fig. 6. In order not to include particles from the nuclear fragmentation, the fitting procedure is only performed in the region $0 \leq \eta \leq y_p$ and only shower particles ($\beta > 0.7$) are considered. From Gaussian fits three parameters are obtained; the position of the distribution, η_{peak} , the height of the distribution, ρ_{max} , and the width of the distribution, σ . These parameters have been studied as a function of energy, centrality and size of the interacting systems.⁵ In a Gaussian representation the integrated multiplicity, n , is given by:

$$n = \sqrt{2\pi} \cdot \sigma \cdot \rho_{max} \quad (3)$$

In Fig. 7 the widths obtained for different subsamples are summarized. Each sample is divided into different centrality bins as given by the impact parameter, Q_{ZD} , i.e. the fraction of non-interacting protons from the projectile. We observe that for a given energy the widths are independent of the size of the interacting systems. When going from peripheral ($Q_{ZD}/Z_{beam} \approx 1$) to central ($Q_{ZD}/Z_{beam} \approx 0$) interactions the widths show only a (10-20)% variation.

The energy dependence on σ is shown in Fig. 8. The variation of σ with energy is simply connected to the available phase space and σ can be parametrized as

$$\sigma = \alpha + \beta \cdot \ln E, \quad (4)$$

with $\alpha=0.51 \pm 0.05$ and $\beta=0.17 \pm 0.01$.¹ For 11.6 A GeV/c we extract the value $\sigma=0.91$ for central events.

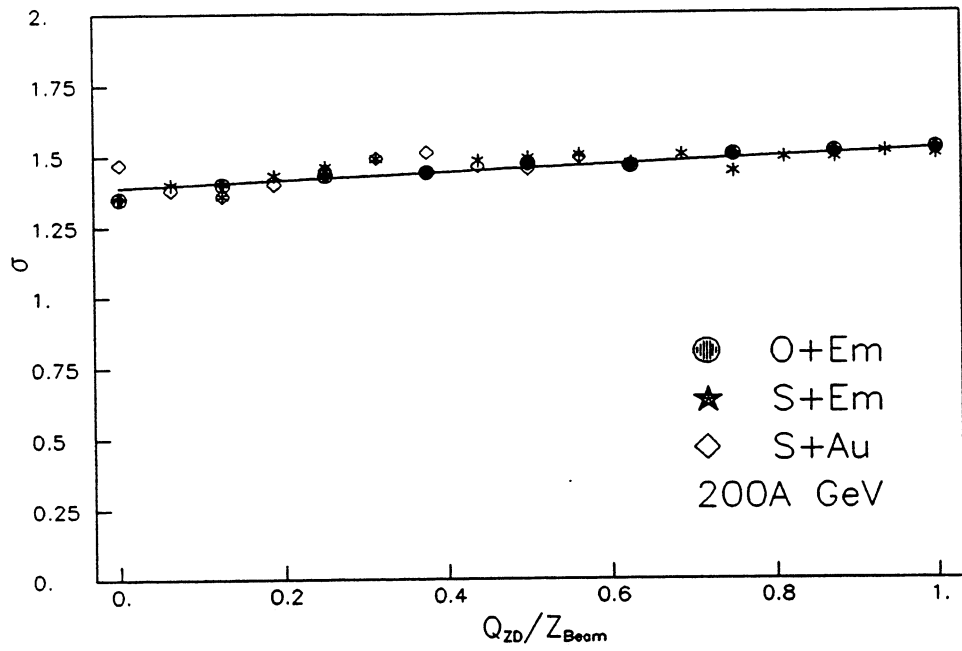


Fig. 7: The dependence between the dispersion, σ , from Gaussian fits, and the centrality parameter Q_{ZD}/Z_{beam} .

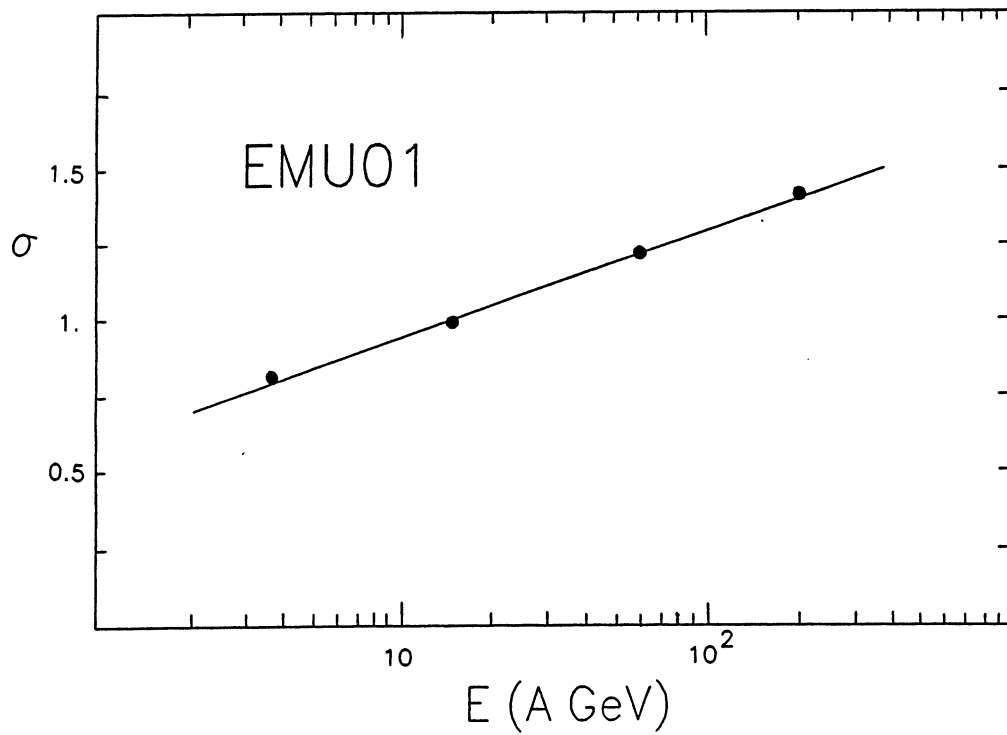


Fig. 8: The energy dependence of the width, σ , of the pseudorapidity distributions for central events.

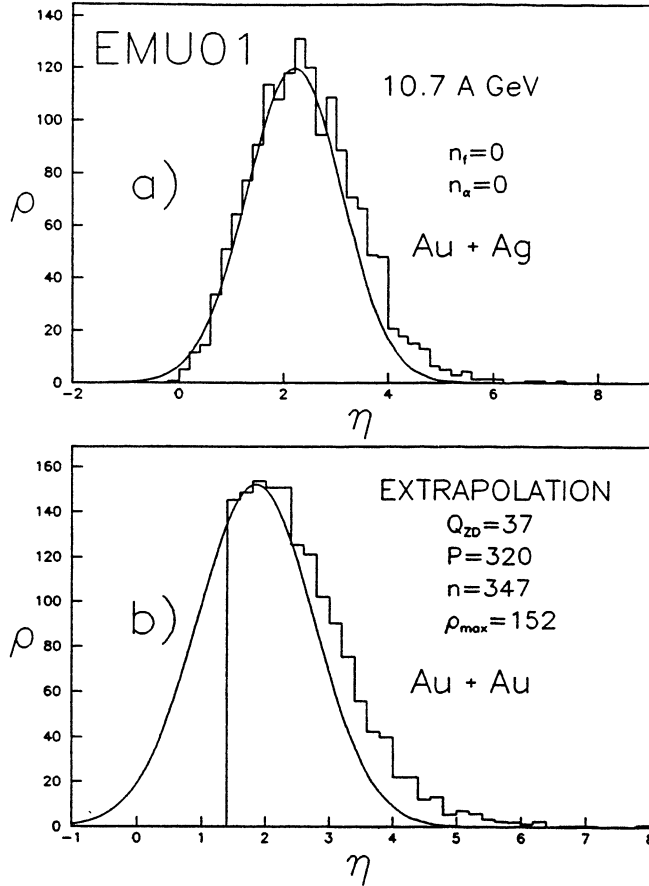


Fig. 9: Pseudorapidity distributions in central a) Au+Ag(Br) and b) Au+Au interactions compared to extrapolated distributions.

8. Extrapolation to Heavier Systems

The regularity of the shape of the pseudorapidity distributions can be used to predict distributions for very heavy systems, e.g. Pb+Pb and Au+Au interactions. These distributions are estimated through the following procedure:

1. Estimate the total multiplicity from Eq. 2 using the pp multiplicity, n_{ch} , at the energy considered and the number of participants, P , for the impact parameters selected by the triggers.

2. Determine η_{peak} from Eq. 1

3. Knowing σ (c.f. Eq. 4) the Gaussian η -distribution is given.

In the next section extrapolated η -distributions are compared to measured distributions in central Au+Au and Au+Ag collisions.

9. Au+Au and Au+Ag interactions at 11.6 A GeV/c

η -distributions of shower particles (singly charged particles with $\beta > 0.7$) have been measured in emulsion chambers (Au+Au) and in emulsion stacks (Au+Ag(Br)). Particle density distributions for central events (complete destruction of the Au projectile into nucleons) are shown in Fig. 9 and compared to the extrapolated distributions. In Au+Ag collisions the particle densities for $\eta \leq \eta_{peak}$ are well described by the extrapolated distribution while an excess of particles are found for $\eta > \eta_{peak}$. Also particle densities in central Au+Au interactions, measured in the chambers only for $\eta > 1.3$, exhibit an excess over

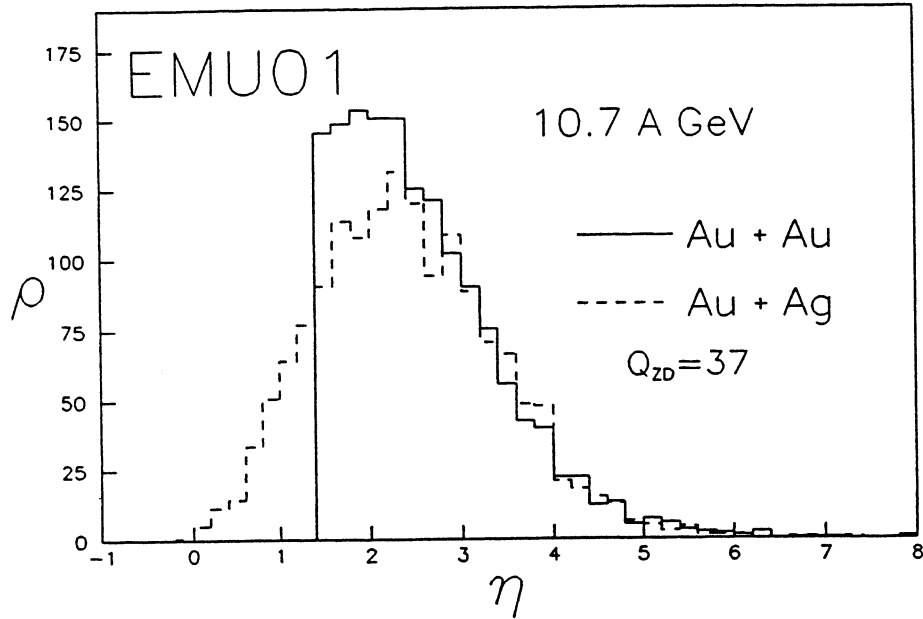


Fig. 10: Comparison between pseudorapidity distributions from Au+Ag and Au+Au interactions with the same values of $\langle Q_{ZD} \rangle$.

the extrapolated distribution for $\eta > \eta_{peak}$. The ρ_{max} -value of 150 is in good agreement with the extrapolation. Contributions from the participant protons to the shower particle multiplicities are different in the η -windows $\eta < \eta_{peak}$ and $\eta > \eta_{peak}$. For $\eta < \eta_{peak}$ no slow participant protons (grey track particles) are counted due to the β -cut ($\beta > 0.7$). On the other hand participant protons from the projectile Au nuclei are included among the shower particles and they appear with $\eta > \eta_{peak}$. This may be the reason for the excess of particles with $\eta > \eta_{peak}$ observed in the measured distributions.

The η -distribution can be divided into three regions; the target fragmentation region, the central region and the projectile fragmentation region. In a participant-spectator picture the particles produced in the projectile and target fragmentation regions depends mainly on the number of projectile participants, (P_P), and target participants, (P_T), respectively. The particle production in the central region depends on both, i.e. on ($P_T + P_P$). To illustrate this we have selected Au+Au and Au+Ag events with the same charge flow in the forward direction, i.e. $\langle Q_{ZD}(Au+Au) \rangle = \langle Q_{ZD}(Au+Ag) \rangle$. In these interactions $\langle P_P \rangle$ could be expected to be the same while the total number of participants are different. The total number of participants, $\langle P_T + P_P \rangle$, were estimated to be 320 and 250 in the Au+Au and Au+Ag interactions, respectively. The measured η -distributions are compared in Fig. 10. As seen the particle densities are the same in the projectile fragmentation region. The ratio of the densities in the central region is 1.25 close to the ratio between the the number of participants which is $\langle P_T + P_P \rangle_{Au+Au} / \langle P_T + P_P \rangle_{Au+Ag} = 320/250 = 1.28$.

10. Fluctuations

Fig. 11 shows the chamber event with the highest multiplicity. Are the fluctuations seen here large or small? In order to judge we have performed a simple estimate of the

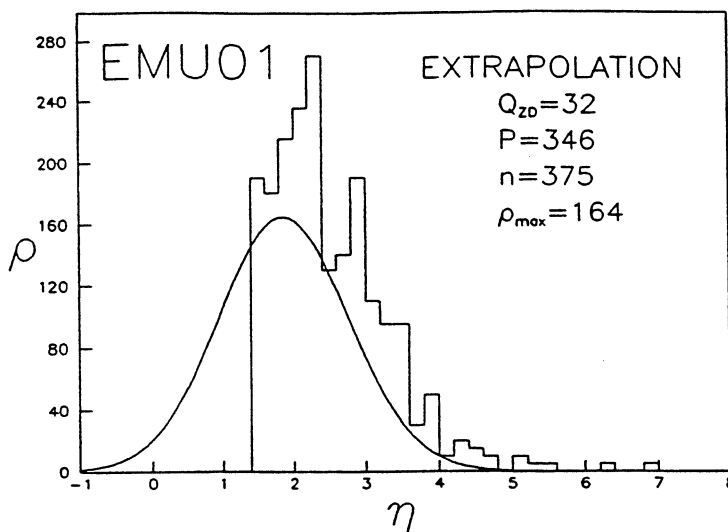


Fig. 11: η -distribution for the Au+Au event with the highest multiplicity

expected fluctuations.

We divide the rapidity window $1.35 < \eta < 2.35$ into bins of $\delta\eta = 0.2, 0.1$ and 0.02 and study the multiplicity distributions in these η -bins. In Fig. 12 the particle density distributions are shown. The source for the fluctuations which we consider here are:

- i) the fluctuations in the number of participants and
- ii) the fluctuations in the particle production from the sources.

We assume each participant nucleon to be a source of particle production. In pp collisions $\sigma(n)/\langle n \rangle = 0.5$, i.e. 50% fluctuations when the number of participants are 2. If we have as many as 300 participants the fluctuations in the number of particles produced per participant (n/P) will then be only $\sim 4\%$. The fluctuations in the number of participants is known to be of the order of 10% and is thus the dominating contribution to the fluctuations. Only fluctuations in P are therefore considered. Taken the global fluctuations to be 10% and assuming stochastic emission we arrive at the distributions shown by the solid curves in Fig. 12. The fluctuations in ρ can fully be understood from this simple estimate and no further contributions to the fluctuations need to be added.

11. Conclusions

The multiplicity of fragments with $Z \geq 3$ and $Z=2$ seems to be similar in Au+Em interactions at AGS (11.6 A GeV/c) and at LBL (900 MeV/c) energies. However the percentage of interactions with complete projectile break-up is higher at AGS energies.

The angular distribution of projectile He-fragments has two components. One could be understood by emission from excited spectators while the other needs more complex production processes.

Shower particle densities in the central and target regions of pseudorapidity are in agreement with extrapolations from light nuclei (O, Si and S) induced interactions studied at AGS and CERN energies.

Fluctuations in particle densities in the central region can be understood from just stochastic emission and fluctuations in the number of participants.

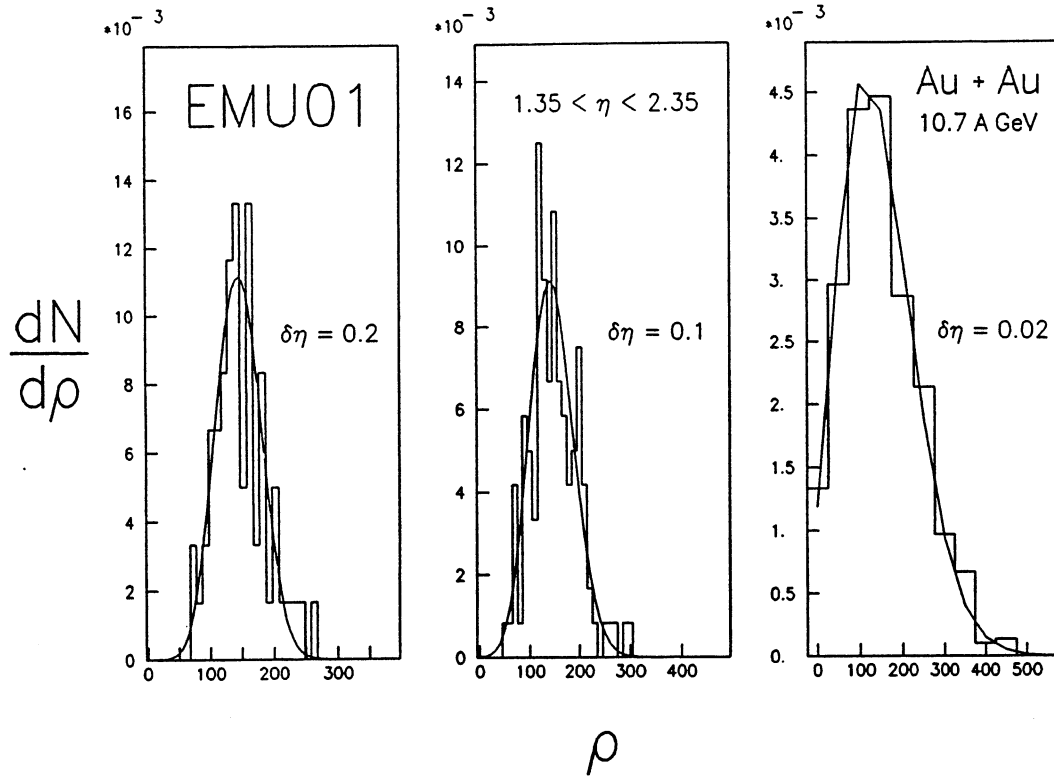


Fig. 12: Particle density distributions in the windows $\delta\eta = 0.2$, 0.1 and 0.02 . The solid curves are from a simple estimate considering stochastic emission and fluctuations in the number of participants.

12. Acknowledgements

The financial support from the Swedish Natural Science Research Council, the German Federal Minister of Research and Technology, the University Grant Commission, the Government of India, the National Science Foundation of China, the Distinguished Teacher Foundation of the State Education Commission of China, the Fok Ying Tung Education, and the US Department of Energy and the National Science Foundation are gratefully acknowledged.

13. References

1. EMU01 collaboration, M. I. Adamovich *et al.*, Phys. Rev. Lett. **69**, 745 (1992)
2. C. J. Waddington and P. S. Freier, Phys. Rev. **C31**, 888 (1985)
3. EMU01 collaboration, E. Stenlund *et al.*, Proc. XXII Int. Symp. on Multiparticle Dynamics, Santiago de Campostella, Spain, 13-17 July 1992
4. B. Nilsson-Almqvist and E. Stenlund, Comp. Phys. Comm. **43**, 387 (1987)
5. EMU01 collaboration, M. I. Adamovich *et al.*, Z. Phys. **C56**, 509 (1992)